Dielectrophoretic label-free immunoassay for rare-analyte quantification in biological samples

Logeeshan Velmanickam, Darrin Laudenbach, and Dharmakeerthi Nawarathna
Department of Electrical and Computer Engineering, North Dakota State University, Fargo, North Dakota, 58102-6050, USA
(Received 15 June 2016; published 11 October 2016)

The current gold standard for detecting or quantifying target analytes from blood samples is the ELISA (enzyme-linked immunosorbent assay). The detection limit of ELISA is about 250 pg/ml. However, to quantify analytes that are related to various stages of tumors including early detection requires detecting well below the current limit of the ELISA test. For example, Interleukin 6 (IL-6) levels of early oral cancer patients are $<$100 pg/ml and the prostate specific antigen level of the early stage of prostate cancer is about 1 ng/ml. Further, it has been reported that there are significantly less than 1 pg/mL of analytes in the early stage of tumors. Therefore, depending on the tumor type and the stage of the tumors, it is required to quantify various levels of analytes ranging from ng/ml to pg/ml. To accommodate these critical needs in the current diagnosis, there is a need for a technique that has a large dynamic range with an ability to detect extremely low levels of target analytes ($<$pg/ml). To address this gap, we here report on a label-free, high-throughput technique based on dielectrophoresis. This technique is capable of quantifying target analytes down to a few thousands of molecules ($\sim$zmoles).

DOI: 10.1103/PhysRevE.94.042408

I. INTRODUCTION

Immunoassays are utilized to detect or quantify target biomolecules such as proteins, antigens, and antibodies in biological samples [1,2]. Typically, in immunoassays, first the specific target antibody is attached onto a solid surface of a device or a traditional well plate. Second, the biological sample that is containing the target molecules (analytes) is pipetted or flowed over the antibodies allowing the analytes to conjugate with antibodies. Finally, the presence of antibody-analyte complexes is detected and the levels of target analytes in the sample can be quantified [2,3]. For example, during the diagnosis of tumors or when monitoring the progress of ongoing treatments for tumors, it is required to monitor the levels of representative tumor markers (proteins) in patients' blood [4,5]. This is typically performed through immunoassays, and the current gold standard for detecting or quantifying target analytes from blood samples is the ELISA (enzyme-linked immunosorbent assay). The ELISA uses antibody-analyte conjugation followed by quantification of antibody-analyte complexes in the sample [5]. The commonly used method for quantifying antibody-analyte complexes involves measuring the concentration (analyte) dependent color change or fluorescence intensity change in the sample. The detection limit of ELISA is about 250 pg/ml [6]. However, to detect or quantify analytes (proteins) that are related to various stages of tumors, including early detection, requires detecting well below the current limit of the ELISA. For example, Interleukin 6 (IL-6) levels of early oral cancer patients are $<$100 pg/ml and the prostate specific antigen (PSA) level of the early stage of prostate cancer is about 1 ng/ml [7]. Further, it has been reported that there are $\ll$pg/mL analytes in the early stage of tumors [7]. Therefore, depending on the tumor type and the stage of the tumors, various levels of analytes ranging from ng/ml to pg/ml must be quantified [6,7]. Furthermore levels of the number of protein targets (typically four to six protein targets) must be detected or quantified in a single experiment [8]. To accommodate these critical needs in the current diagnosis, there is a need for a technique that has a large dynamic range with an ability to detect extremely low levels of target analytes ($<$pg/ml).

To address this critical need in biology and medicine, a number of new techniques have been proposed and utilized. Among the new techniques, impedimetric based analyte detection or quantification offers a low cost and label-free technique [8–11]. It uses an array of microelectrodes called interdigitated electrodes that are fabricated on glass or similar materials [12–14]. In impedimetric experiments, the change of impedance upon binding the target analytes onto antibodies that are immobilized on the electrodes or between electrodes is measured at low frequencies ($<$1000 Hz). Using a standard curve of known analyte concentration vs change in impedance, the unknown analyte concentrations are calculated [13]. It has been reported that the lowest analyte concentration that can detect or quantify using this technique is about 80 pg/ml [8]. However, impedimetric based analyte detection or quantification suffers a number of limitations, such as the following: Impedance is dependent on the conductivity of the biological sample, there is need for expensive electric circuits and equipment (impedance analyzers) to record the impedance, and impedance varies from one analyte type to another. In addition to impedimetric based detection or quantification, there are number of other techniques such as ion sensitive field-effect transistors, semiconducting carbon nanotubes, thin-film gate transistors, and electrolyte-insulator-semiconductor structures that are available to detect or quantify target analytes of a sample [8,15]. However, almost all of these techniques require target analytes in very low ionic buffer solutions. Therefore, these techniques have been used in applications such as detecting DNA molecules and DNA hybridization events in low-conductivity buffers. Furthermore, it has also been reported that successful development of these techniques for DNA analysis is much complex than expected. In particular, the theoretical basis of the observed results, including a wide variety of reported signal amplitudes and response times, still remains unclear [15]. Therefore, these techniques have very limited applicability in immunoassays. To address this gap, we report here on a label-free, high-throughput technique that is capable of detecting or quantifying target analytes down to few thousands of molecules ($\sim$zmoles). Furthermore, our technique can be integrated with microfluidics chips for

 ©2016 American Physical Society

developing *point-of-care* diagnosis. Our technique utilizes the interaction between antibody-analyte complexes with externally applied electric fields. Moreover, it uses frequency dependent dielectrophoresis (DEP) to detect and quantify analytes.

II. THEORY

The DEP is the motion of particles that are suspended in a medium relative to the medium [16–19]. The DEP results from polarization forces. If a uniform electric field is applied to a dielectric homogeneous particle, it will be polarized but will stay without any movement. Similarly, if a nonuniform electric field is applied to the particle, it will start moving toward the highest electric field strength region (and also to the highest field gradient) or lowest electric field strength region (and also to the lowest field gradient), depending on its polarization [16–19].

Mathematically, the magnitude of the time-average DEP force acting on a homogeneous isentropic dielectric spherical particle in a nonuniform electric field can be represented by

$$|F_{\mathrm{DEP}}| = 2\pi r^3 \varepsilon_m \mathrm{Re}[f_{\mathrm{CM}}(\omega)]|\nabla(E^2)|, \tag{1}$$

where ∇ is the vector operator, $\boldsymbol{E}$ is the rms electric field, r is the radius of the spherical dielectric particle, ε_m is the permittivity of the suspending medium, ω is the radial frequency of the applied electric field, and $\mathrm{Re}\{f_{\mathrm{CM}}(\omega)\}$ is the real part of the Clausius-Mossotti factor (CM), and is defined as

$$f_{\mathrm{CM}}(\omega) = (\varepsilon_p^* - \varepsilon_m^*)/(\varepsilon_p^* + 2\varepsilon_m^*), \tag{2}$$

where ε_p^* is the complex permittivity of the dielectric particle and ε_m^* is the complex permittivity of the suspending medium [16–20]. The complex permittivity is given by $\varepsilon^* = \varepsilon - j(\frac{\sigma}{\omega})$ with σ the real conductivity, ε the real permittivity, and ω the angular frequency [16–20]. The real part of the CM factor is theoretically bounded between $-1/2$ and 1. Further, it determines the direction and the relative strength of the DEP force. If $\mathrm{Re}\{f_{\mathrm{CM}}(\omega)\}$ becomes zero under certain conditions, the dielectrophoretic force acting on the polarized particles also becomes zero. This zero force frequency is called crossover frequency (f_{CO}), which is defined as

$$f_{\mathrm{CO}} = \frac{1}{\varepsilon_0 2\pi}\sqrt{-\frac{(\sigma_p - \sigma_m)(\sigma_p + 2\sigma_m)}{(\varepsilon_p - \varepsilon_m)(\varepsilon_p + 2\varepsilon_m)}}, \tag{3}$$

where σ,ε are the real conductivity and relative permittivity, and subindices p,m are the particle and medium, respectively [20]. It has been demonstrated that f_{co} depends on the conductivity (σ_p) of the particle at low frequencies (<1 MHz) [20]. The conductivity (σ_p) of the homogeneous dielectric spherical particle can be written as the sum of bulk conductivity ($\sigma_{p\mathrm{bulk}}$) and surface conductance (K_S), which can be represented as

$$\sigma_p = \sigma_{p\mathrm{bulk}} + \frac{2K_S}{r}, \tag{4}$$

where r is the radius of the spherical particle. Depending on the material of the particle, for example, polystyrene and silica, the bulk conductivity ($\sigma_{p\mathrm{bulk}}$) can be negligible; therefore surface conductance (K_S) provides a dominating contribution to the conductivity of the particle [20]. At higher frequencies (>1 MHz), f_{CO} depends on the permittivity of the particle (ε_p) [20]. From these equations, it can be concluded that, at low frequencies, crossover frequency is dependent on the surface conductance. We have utilized crossover frequency as our method of detection or quantification of various levels of target analytes in biological samples. Moreover, we have utilized the polystyrene beads having modified the surfaces with antibodies that are selectively conjugating with target analytes. We then mixed the beads and the sample to conjugate the antibodies and target analytes. After conjugation, we resuspended the polystyrene beads in a testing buffer (this will be discussed in detail below) and measured the crossover frequency. As predicted in the theoretical calculations above, our data indicate that crossover frequency is dependent on the number of antibody-analyte complexes on the polystyrene beads' surfaces. We have found a relationship between crossover frequency and the number of avidin-biotin conjugates, which can be used as a standard curve to find the number of avidin molecules in unknown samples. Therefore, this technique can be utilized to quantify an unknown level of target analytes in a biological sample. Our experiments were performed using the avidin molecules that are suspended in standard laboratory buffers. However, in real-world applications where we apply this concept, for example, to find the molarity of biomarker proteins in blood, the results will not be affected by the nonspecific binding of other molecules. This is because the crossover frequency is dependent on the polarization of biotin-avidin or (analyte-antibody) with the applied electric field. If there is nonspecific binding, depending on the number of nonspecific molecules, it may produce a crossover frequency that is outside the standard curve generated for specific analyte-antibody conjugation. Furthermore, near the crossover frequency, DEP is very small and polystyrene beads will scatter from the Brownian motion. However, this happen when polystyrene beads are extremely close to the crossover frequency. Therefore error estimating crossover frequency is very small. Prior to our studies, Gagnon and co-workers used the crossover frequency to detect the DNA hybridization on polystyrene beads [21]. We used their work as the basis for our work. In particular, we have designed and used a unique set of electrodes that can be used to easily identify the positive, negative, and zero DEP forces. In addition, we have detected and quantified the conjugation of low amounts of biotin-avidin conjugates. We have also studied the variation of the crossover frequency with the number of biotin-avidin conjugates. In comparison with Gagnon's work, detecting protein binding events is extremely useful in biology and medicine, more so than DNA hybridization. At the same time it is technically challenging to detect the protein binding without the electrodes that we have developed. Further, our work is a demonstration of DEP based label-free ELISA. We will next explain the details of the experiments that we performed.

III. THEORETICAL CALCULATIONS

To properly implement our concept in experiments, first, we have designed an electrode array that is capable of detecting DEP forces [positive DEP, negative DEP, or zero DEP

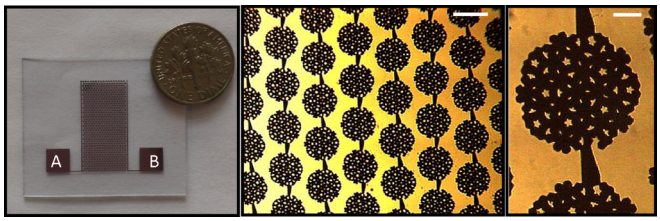

FIG. 1. Pictures of the PIDE electrodes utilized in crossover frequency measurement experiments. (a) A picture of a clean PIDE structure with connecting pads (A and B) to connect the electrodes to external function generator. (b) Section of PIDE structures showing how individual bead electrodes are placed, a gap between the electrodes and a connection between individual bead electrodes. Scale bar indicates 500 μm. (c) Closeup of the single-bead electrode showing a hollow interior with uneven outer boundaries to generate large electric field gradients. Scale bar indicates 250 μm.

(crossover frequency)] of polystyrene beads through simple bright field microscopy observation. We then successfully fabricated the electrode arrays on commercially available glass wafers using traditional photolithography, metal sputtering, and lift-off procedures [22]. All the electrodes were fabricated using 1000-Å-thick gold films.

We have designed pearl-shaped interdigitated electrodes (PIDEs) for crossover frequency experiments (Fig. 1). In comparison with traditional interdigitated electrodes, PIDE electrodes are capable of generating high electric field gradients (∇E^2). Typical interdigitated electrodes generate electric field gradients in the range of 10^{12} V^2/m^3 [16]. However, our PIDE electrodes are generating about 2–3 times higher electric field gradients than the traditional interdigitated electrodes. These high electric field gradients are necessary for quickly detecting DEP forces of polystyrene beads for our high-throughput label-free immunoassay. In particular, depending on the frequency and the surface charges of the polystyrene beads, these high electric field gradients are capable of establishing extremely high negative or positive DEP forces on polystyrene beads allowing a clear distinction between them. Further, other forces acting on the beads such as viscous drag and buoyancy forces are much smaller than the DEP forces. Therefore, DEP forces are easily detectable. In addition, PIDEs have designated regions for positive and negative DEP, where beads will be accumulated. Therefore, it is easy to characterize the DEP forces (+ or -DEP).

To quantitatively understand the electric fields and electric field gradients (∇E^2) generated by PIDE structures, we have utilized the commercially available COMSOL (COMSOL, Inc.) software and calculated the electric field and electric field gradients that we can expect from the PIDE structures. To set up COMSOL calculations, briefly, PIDEs were drawn to a scale using AUTOCAD (AUTODESK) software and imported into COMSOL software. We then used the ac/dc electric current (ec) module and frequency domain studies to calculate electric fields and field gradients. Furthermore, we assumed that a buffer solution ($\sigma = 1.67$ S/m and $\varepsilon_r = 80.3$) was filled over the electrodes. Further, an external potential (1 $V_{peak-peak}$) with a known frequency was applied to the electrodes and the electrode design was meshed using free triangular, extremely fine mesh with a maximum element size of 10 µm and minimum element size of 0.21 µm. Finally, we calculated the electric fields and field gradients for each frequency. Figure 2 illustrates the summary of the electric fields and field gradient calculations. Figure 2(a) indicates the electric fields generated by an external electric potential of 120 kHz on PIDE structures. Large electric fields are necessary to polarize polystyrene beads and generate DEP forces on polystyrene beads. Our electrodes are capable of generating a maximum electric field of 1.8×10^4 V/m and this electric field is sufficient to polarize the polystyrene beads. Figure 2(b) indicates

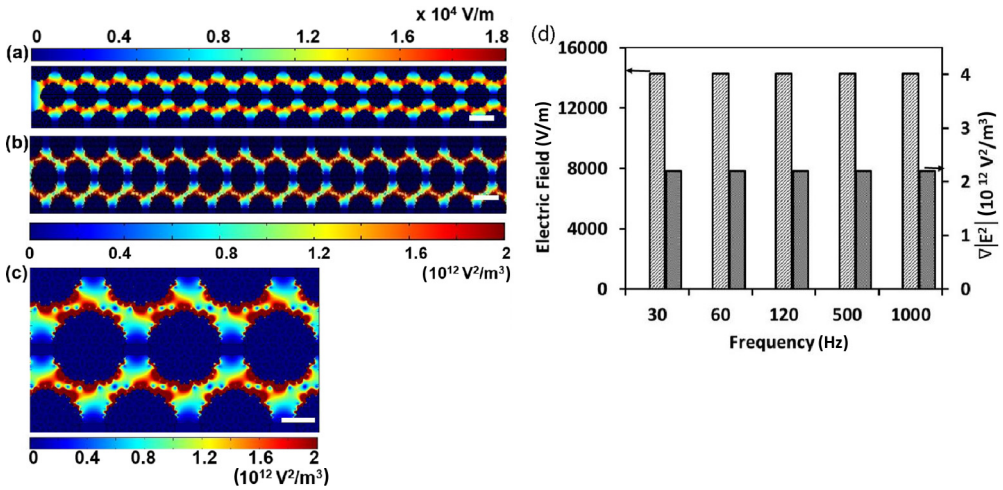

FIG. 2. COMSOL simulations results. (a) Variation of the electric field at 120 kHz over PIDE electrodes. These electric fields are sufficient to polarize the polystyrene beads and generate DEP forces. (b) Calculated electric field gradients (∇E^2) at 120 kHz over the PIDE electrodes. Both electric field and electric field gradients are necessary to set up DEP forces on the beads. (c) Closeup view of the electric field gradient (∇E^2) showing high and low electric field gradient regions in PIDE structures. When polystyrene beads are experiencing attaching or positive DEP, they are attracted to the high field gradient regions. Polystyrene beads move to the lowest field gradient regions when they experience negative DEP. (d) Variation of the average electric field and electric field gradients (∇E^2) with frequency. Scale bars indicate 500 μm in (a,b), 250 μm in (c).

the variation of the electric field gradient (∇E^2) near PIDE structures. These electric field gradients were calculated for 120 kHz external electric potential. Figure 2(c) shows the high and low electric field gradient regions (positive and negative DEP forces). Blue colored regions are negative DEP regions because of the lowest electric field gradient ($\sim 10^{11}$ V^2/m^3). The red colored regions are the positive DEP regions because of the highest electric field gradients ($\sim 3 \times 10^{12}$ V^2/m^3). Figure 2(d) illustrates the variation of the average electric fields and electric field gradients with frequency. As expected, there is no variation with the frequency. Therefore, it can be concluded that polystyrene beads are subjected to the same electric fields and field gradients in all frequencies and the variations in crossover frequency are dependent on the number of analyte molecules on the bead surfaces.

IV. EXPERIMENTS AND RESULTS

To demonstrate the proof of concept of our technique, we have used biotin-avidin conjugations. In particular, we studied the variation of crossover frequency with biotin-avidin conjugates on the polystyrene beads' surfaces. Briefly, biotinylated polystyrene beads were purchased from Spherotech Inc. (0.74-μm-diameter beads; 10 000 biotin molecules in the beads' surfaces). To conjugate avidin molecules (Vector Labs, Inc, $\sim 1.1 \times 10^6$ beads/μl, fluorescently labeled avidin molecules) with biotin molecules that are on the surfaces of the polystyrene beads, we followed the manufacturer's suggested procedure. Briefly, to have 100% (meaning 10 000 molecules) biotin molecules to be conjugated with avidin molecules, we incubated 3 μl of avidin solution (1 mg/ml) and 10-μl polystyrene beads for 30 min at room temperature. We then centrifuged the bead mixture at 5000 rpm for 12 min and the supernatant was removed and 400 μl of testing buffer was added to the sample. We then pipetted 10 μl (8×10^{11} beads/μl) of polystyrene beads onto the commercially available glass slide and recorded a fluorescent image of the sample. The fluorescent intensity of the sample was measured using fluorescent imaging and the IMAGEJ software. Similarly, to have 75%, 50%, 25%, 12.5% and 6.25% conjugations, we diluted the avidin solution appropriately and kept the other experimental parameters (incubation time, temperature, and centrifuge speed) unchanged. Figure 4(a) indicates the variation of the measured fluorescence with avidin molecules. As we expected, the fluorescence intensity gradually increases with the number of avidin molecules.

The crossover experiments were performed in the following manner. First, clean PIDE electrodes were mounted on a low-power microscope (OMFL600). We then pipetted 10 μl of biotin-avidin conjugated beads over the PIDE electrodes. We then connected the PIDE electrodes to a commercially available function generator (HP 33120A). During the crossover measurement experiments, we first established the positive DEP by applying a low-frequency electric field (~10 kHz). Reports in the literature, and our experiments, indicate that polystyrene beads experience positive DEP force at lower frequencies (<50 kHz) [16–18]. We have applied a low-frequency electric field (~10 kHz) and observed the positive DEP. Since the positive DEP is always causing the beads to be attracted toward electrodes, we observed it very clearly [Fig. 3(a)]. We then switched the frequency and observed the negative DEP. Since the positive DEP is in the low frequency, the negative DEP must be in the high frequencies. The highest frequency that our generator can produce is 10 MHz; we started with the highest frequency. During the negative DEP, beads must be repelled from the electrodes and move into the region where it has the lowest electric field gradient. Since we are changing the frequency from 10 kHz to 10 MHz, we were able to observe the repelling of the beads from the electrodes. These steps are shown in Fig. 3(b). After establishing the negative and positive DEP regions, the crossover frequency must be between those two regions. At the crossover frequency, beads do not experience any DEP force; therefore it will scatter randomly through Brownian motion [Fig. 3(c)]. To locate the crossover frequency, we have used a simple binary search algorithm. Briefly, we calculated the average of the two frequencies (10 kHz and 10 MHz, average = 505 kHz) and applied the new frequency and observe the DEP (whether positive or negative). If the DEP was negative, we took a new average between 10 and 505 kHz. Similarly, if the DEP is negative, we took a new average between 505 kHz and 10 MHz. We continued this process and located the crossover frequency. Figure 3 illustrates the implementation of these steps in experiments. In particular, PIDEs provide regions where positive, negative, and crossover DEP forces are easily detectable. Therefore, there is no need to have complex circuitry or algorithms. Typically, it takes about 45–60 min to manually find the crossover frequency of a polystyrene bead sample that has a certain number of avidin molecules. This

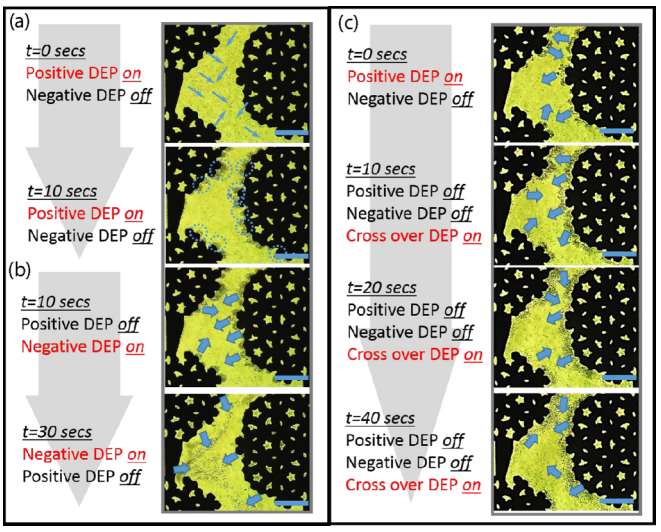

FIG. 3. Experimental scheme used to find the crossover frequency of a sample of polystyrene beads. The moving directions of polystyrene beads under various frequencies are indicated by arrows. (a) Experimental observation of positive DEP. During the positive DEP, polystyrene beads are moving to the highest electric field gradient (∇E^2) regions. (b) Observation of negative DEP. Note that the polystyrene beads are moving to the lowest electric field gradient (∇E^2) regions (away from the electrodes). (c) Polystyrene beads are transitioning from positive DEP to crossover DEP. Note that at crossover frequency, polystyrene beads are gradually scattering over the PIDE electrodes. Scale bars indicate 100 μm.

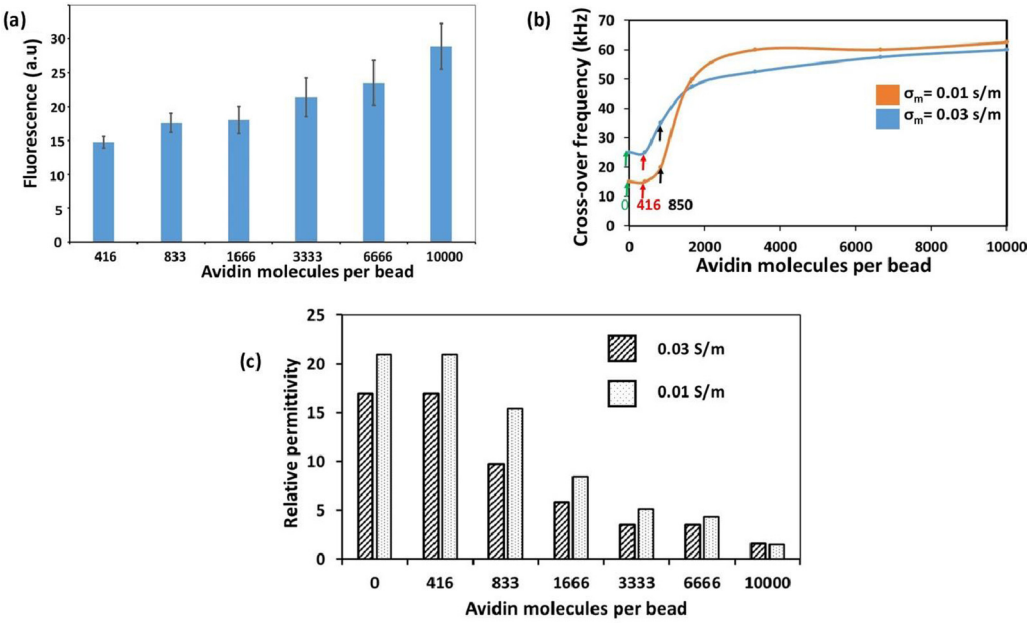

FIG. 4. Experimental and theoretical results. (a) Variation of the fluorescence intensity of polystyrene beads with a number of fluorescently labeled avidin molecules on their surfaces. (b) Experimentally measured crossover frequency of the polystyrene beads with avidin molecules on the surfaces. (c) Calculated relative dielectric constant of polystyrene beads with varying number of avidin molecules. This calculation was performed using the experimental data in (b).

timing can be significantly reduced down to minutes through automation. Figure 3(a) demonstrates how we determined the positive DEP of a sample. In positive DEP, note that polystyrene beads are getting collected in the high electric field gradient region as expected. As shown in Fig. 3(b), during the negative DEP, polystyrene beads get collect in the lowest electric field gradient regions. At the crossover frequency, there was no DEP force acting on the polystyrene beads; therefore the beads are free to move in any direction over the PIDE electrodes [Fig. 3(c)]. Figure 3(c) illustrates how the beads are gradually scattering over electrodes at the crossover frequency. This experimental procedure was utilized to experimentally find the crossover frequency of polystyrene beads with avidin molecules on their surfaces. In addition, we have also repeated each experiment 2–3 times for repeatability.

To study the applicability of our techniques in low- and high-conductivity buffers, we have performed the crossover frequency experiments in two separate buffers ($\sigma_1 = 0.03$ and $\sigma_2 = 0.01$ S/m). Conductivity, σ_1, is comparable with common phosphate buffered saline (PBS). PBS buffer was diluted 100× in DI water and used as the low-conductivity buffer (σ_2) in our experiments. Figure 4(b) shows the average crossover frequency (averaged using 2–3 experiments) for each condition (number of avidin molecules). The crossover frequencies for zero and 460 avidin molecules are identical [Fig. 4(a) red and green arrows] and therefore 460 avidin molecules cannot be quantified. From these experimental evidences, it can be concluded that our crossover frequency based quantification can quantify about 850 molecules (smallest bead quantity) per polystyrene bead (∼1.4 zmoles per bead). The number of beads was calculated in the following manner; for 100% biotin-avidin conjugation in a bead, there will be 10 000 avidin molecules on a single bead surface. To cover 8.33% of the beads' surface, there should be about 850 avidin molecules in a single bead surface. Furthermore, the crossover frequency of the polystyrene beads is dependent on the number of avidin molecules on the bead surfaces and the conductivity of the buffer solutions. These variations can be explained theoretically using the expression derived for the crossover frequency [Eq. (4)]. To demonstrate the applicability of our technique in sensing applications in various biological buffers, we have plotted the variation of the crossover frequency with the number of biotin-avid conjugates [Fig. 4(b)] and generated a standard curve. This standard curve can be used to find the number of avidin molecules of an unknown experiment.

The dielectric properties (conductivity or the dielectric constant) of the polystyrene beads strongly contribute to the crossover frequency [16–18]. Since the crossover frequencies of polystyrene beads with avidin molecules were below 1 MHz [Fig. 4(b)], we were interested in finding how surface conductivities (surface conductivity is closely related to the biotin-avidin conjugation) and relative dielectric constants contribute to the measured crossover frequencies. However, surface conductance is closely related to the biotin-avidin conjugation as it determines the property of beads with biotin-avidin molecules. We first calculated the variation in the surface conductance of beads at crossover frequencies. To calculate the surface conductance, we have utilized Eqs. (4) and (5) in Ref. [21] with $\varepsilon_m = 80.3$, $\varepsilon_p = 2.6$, and $\sigma_m = 0.03, 0.01$ S/m. From our calculation, we found that there is no change in surface conductance of polystyrene beads (K_s) and the value of the surface conductance is about 6.16 nS in all the experiments. We then calculated the ε_p at each crossover frequency and those results are indicated in Fig. 4(c). Since there is a significant variation in the dielectric constant from experiment to experiment, from these calculations, it can be

concluded that avidin binding to the biotin molecules on the beads' surfaces is reflected as a change in dielectric constant.

V. CONCLUSIONS

In summary, we have proposed a concept for developing label-free immunoassays. In addition to addressing the current technological gap in immunoassay, this technique can be developed into a *point-of-care* technology for quickly detecting other diseases such as myocardial infarctions (heart attacks) and infections. These diseases are demanding high-throughput techniques. In addition, single-cell biology is a rapidly growing area of biology. In particular, single-cell genomics studies have been utilized to understand the complicated biological process taking place in tumors, the brain, and wound healing. It is expected that single-cell biology is proposed to be utilized in developing effective diagnoses. Due to lack of techniques, current single-cell studies are limited to RNA sequencing and there is a demand for high-throughput single-cell proteomics analysis of single cells. Since our proposed technique is capable of quantifying a few thousands of analytes (zmoles per bead), this can be developed to perform single-cell proteomics. To successfully implement, our technique must be integrated with microfluidics device design and instrumentation. Therefore, the research presented here holds great promise in many important areas of biology and medicine.

ACKNOWLEDGMENTS

We would like to thank Jeffery Erickson and Vidura Jayasooriya in the Electrical and Computer Engineering Department at the North Dakota State University for their help in experiments. We also thank the staff of the Center for Nanoscience and Engineering at the North Dakota State University for their help in fabricating electrodes used in experiments.

[1] C. N. Hales and P. J. Randle, Biochem. J. **88**, 137 (1963).
[2] H. Magdelenat, S. Merle, and A. Zajdela, Cancer Res. **46** (Suppl. 8), 4265s (1986).
[3] R. S. Yalow and S. A. Berson, Obes. Res. **4**, 583 (1996).
[4] J. Wu, Z. Fu, F. Yan, and H. Ju, TrAC, Trends Anal. Chem. **26**, 679 (2007).
[5] H. Chen, C. Jiang, C. Yu, S. Zhang, B. Liu, and J. Kong, Biosens. Bioelectron. **24**, 3399 (2009).
[6] B. V. Chikkaveeraiah, A. A. Bhirde, N. Y. Morgan, H. S. Eden, and X. Chen, ACS Nano **6**, 6546 (2012).
[7] J. F. Rusling, C. V. Kumar, J. S. Gutkind, and V. Patel, Analyst **135**, 2496 (2010).
[8] J. S. Daniels and N. Pourmand, Electroanalysis **19**, 1239 (2007).
[9] M. C. Rodriguez, A. N. Kawde, and J. Wang, J. Chem. Soc., Chem. Commun. **34**, 4267 (2005).
[10] M. Varshney, Y. Li, B. Srinivasan, and S. Tung, Sens. Actuators, B **128**, 99 (2007).
[11] H. Cai, T. M. H. Lee, and I. M. Hsing, Sens. Actuators, B **114**, 433 (2006).
[12] Z. Zou, J. Kai, M. J. Rust, J. Han, and C. H. Ahn, Sens. Actuators, A **136**, 518 (2007).
[13] D. Xu, D. Xu, X. Yu, Z. Liu, W. He, and Z. Ma, Anal. Chem. **77**, 5107 (2005).
[14] D. Berdat, A. C. M. Rodríguez, F. Herrera, and M. A. Gijs, Lab Chip **8**, 302 (2008).
[15] A. Poghossian, A. Cherstvy, S. Ingebrandt, A. Offenhäusser, and M. J. Schöning, Sens. Actuators, B **111**, 470 (2005).
[16] R. Pethig, Biomicrofluidics **4**, 022811 (2010).
[17] N. G. Green and H. Morgan, J. Phys. Chem. B **103**, 41 (1999).
[18] A. Castellanos, A. Ramos, A. Gonzalez, N. G. Green, and H. Morgan, J. Phys. D: Appl. Phys. **36**, 2584 (2003).
[19] R. Zhou, P. Wang, and H. C. Chang, Electrophoresis **27**, 1376 (2006).
[20] L. Cui, D. Holmes, and H. Morgan, Electrophoresis **22**, 3893 (2001).
[21] Z. Gagnon, S. Senapati, J. Gordon, and H. C. Chang, Electrophoresis **29**, 4808 (2008).
[22] R. S. Martin, A. J. Gawron, S. M. Lunte, and C. S. Henry, Anal. Chem. **72**, 3196 (2000).